Journal of Solid Mechanics Vol. 8, No. 3 (2016) pp. 662-678

Free Vibration Analysis of Variable Stiffness Composite Laminates with Flat and Folded Shapes

B. Daraei , S. Hatami *

Civil Engineering Department, Yasouj University, Yasouj, Iran

Received 27 June 2016; accepted 29 August 2016

ABSTRACT

In this article, free vibration analysis of variable stiffness composite laminate (VSCL) plates with flat and folded shapes is studied. In order to consider the concept of variable stiffness, in each layer of these composite laminated plates, the curvilinear fibers are used instead of straight fibers. The analysis is based on a semi-analytical finite strip method which follows classical laminated plate theory (CLPT). Natural frequencies obtained through this analysis for the flat plates are in good agreement with the results obtained through other methods. Finally, the effect of the fiber orientation angle, the folding order, crank angles and boundary conditions on the Natural frequencies is demonstrated.

Keywords : Vibration; Variable stiffness composite laminates; Finite strip method; Classical laminated plate theory; Laminated folded plate.

1 INTRODUCTION

FIBER reinforced composite laminates can have many advantages, such as high strength-to-weight ratio and high corrosion resistance. A lamina or ply is a typical sheet consisting of a reinforcing fiber imbedded in a matrix and a laminate made up of a series of laminas. In a constant stiffness composite laminate (CSCL), layers have straight fibers, whereas in a variable stiffness composite laminate (VSCL), they have curvilinear fibers. In VSCL plates, since fiber orientation at any point can be different, plate stiffness could vary accordingly. Use of VSCL instead of CSCL, can increase or decrease the natural frequencies and avoid vibrational resonance [1].

Folded plates are assemblies of flat plates rigidly connected together along their edges. Folded plate structures are easy to form and are economical compared with other shells (such as cylindrical ones). These structures can have applications in aircraft fuselage.

In the following section, an attempt is made to touch upon previous studies into VSCL flat plates.

In 2008, Gürdal et al. [2] analyzed variable stiffness panels for in-plane and buckling responses. In 2011, Akhavan and Ribeiro [1] analyzed VSCL plates for natural frequencies and vibrational mode shapes, using finite element method. They investigated the effects of using curvilinear fibers instead of straight fibers on the mode shapes and natural frequencies of vibration. They found that using VSCL plates can change mode shapes of vibration meaningfully and may lead to a significant decrease or increase in the natural frequencies. In 2012, Ribeiro and Akhavan [3] analyzed non-linear vibrations of VSCL plates using finite element method. In 2013, Akhavan et al. [4] studied large deflection and stresses of VSCL plates using finite element method. In 2013, Houmat [5] studied nonlinear free vibration of fully clamped VSCL plates using finite element method. In 2014, Yazdani et al. [6] analyzed linear and non-linear deflections of VSCL plates using finite element method. In 2014, Akbarzadeh et al. [7] studied static bending, buckling, and free vibration of VSCL plates. They first presented the governing equations

*Corresponding author. Tel.: +98 7431005118; Fax: +98 7433221711.
E-mail address: hatami@yu.ac.ir (S.Hatami).

obtained via classical and shear deformation theories, and then solved them by using the hybrid Fourier-Galerkin Method. In 2015, Yazdani and Ribeiro [8] studied free vibration analysis of thick VSCL plates using finite element method.

Because there is no data in the field about the analysis VSCL folded plates, in this article, free vibration analysis of VSCL flat and folded plates is studied.

2 THEORY

Here, a laminated composite of total thickness h composed of n layers with length L and width b is considered. In addition, application is made of X and Y and Z Cartesian coordinates system. XY-plane is taken in the mid-plane of the laminate. For the purpose of considering the variable stiffness, it is assumed that the orientation of the reference fiber path in each layer changes linearly with respect to the X coordinate and is defined as:

$$\theta(X)=\frac{2(T_1-T_0)}{L}\left|X-\frac{L}{2}\right|+T_0 \tag{1}$$

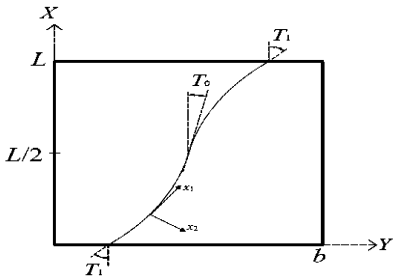

Fig.1
Fiber orientation in a layer of VSCL.

T_0 is the path orientation in X=L/2, T_1 is the path orientation in X=0 and X=L (Fig. 1). The remaining paths can be found by shifting the reference fiber path along the Y axis. Here, the ply angle for a layer of VSCL is defined as $\langle T_0/T_1\rangle$. For example, a two-layer VSCL with stacking sequence $[\langle 30/60\rangle,\langle -30/-60\rangle]$ means two layer VSCL with $T_0=30°, T_1=60°$ in the first layer and $T_0=-30°, T_1=-60°$ in the second layer (Fig. 2).

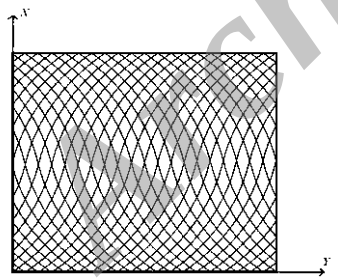

Fig.2
Two-layer VSCL with stacking sequence $[\langle 30/60\rangle,\langle -30/-60\rangle]$.

2.1 Theory of VSCL plates

To write the stress-strain relations, classical laminated plate theory has been used. According to this theory, the displacements are as follows [9]:

$$\begin{aligned} u(X,Y,Z,t)&=u_0(X,Y,t)-Z\frac{\partial w_0}{\partial X}\\ v(X,Y,Z,t)&=v_0(X,Y,t)-Z\frac{\partial w_0}{\partial Y}\\ w(X,Y,Z,t)&=w_0(X,Y,t)\end{aligned} \tag{2}$$

where u, v and w are the displacements in the X, Y, and Z directions respectively, and u_0, v_0 and w_0 are the values of u, v, and w at the mid-plane, respectively. The strain–displacement relations can be written as [9]:

$$\begin{Bmatrix} \varepsilon_{XX} \\ \varepsilon_{YY} \\ \gamma_{XY} \end{Bmatrix} = \begin{Bmatrix} \varepsilon^{(0)}{}_{XX} \\ \varepsilon^{(0)}{}_{YY} \\ \gamma^{(0)}{}_{XY} \end{Bmatrix} + Z \begin{Bmatrix} \varepsilon^{(1)}{}_{XX} \\ \varepsilon^{(1)}{}_{YY} \\ \gamma^{(1)}{}_{XY} \end{Bmatrix} \tag{3}$$

where

$$\left\{\varepsilon^0\right\} = \begin{Bmatrix} \varepsilon^{(0)}{}_{XX} \\ \varepsilon^{(0)}{}_{YY} \\ \gamma^{(0)}{}_{XY} \end{Bmatrix} = \begin{Bmatrix} \dfrac{\partial u_0}{\partial X} + \frac{1}{2}\left(\dfrac{\partial w_0}{\partial X}\right)^2 \\ \dfrac{\partial v_0}{\partial Y} + \frac{1}{2}\left(\dfrac{\partial w_0}{\partial Y}\right)^2 \\ \dfrac{\partial u_0}{\partial Y} + \dfrac{\partial v_0}{\partial X} + \dfrac{\partial w_0}{\partial X}\dfrac{\partial w_0}{\partial Y} \end{Bmatrix} \tag{4}$$

$$\left\{\varepsilon^1\right\} = \begin{Bmatrix} \varepsilon^{(1)}{}_{XX} \\ \varepsilon^{(1)}{}_{YY} \\ \gamma^{(1)}{}_{XY} \end{Bmatrix} = \begin{Bmatrix} -\dfrac{\partial^2 w_0}{\partial X^2} \\ -\dfrac{\partial^2 w_0}{\partial Y^2} \\ -2\dfrac{\partial^2 w_0}{\partial X\,\partial Y} \end{Bmatrix} \tag{5}$$

$(\varepsilon^{(0)}{}_{XX}, \varepsilon^{(0)}{}_{YY}, \gamma^{(0)}{}_{XY})$ are the membrane strains, and $(\varepsilon^{(1)}{}_{XX}, \varepsilon^{(1)}{}_{YY}, \gamma^{(1)}{}_{XY})$ are the mid-plane curvatures. Like a CSCL plate, in a VSCL plate, layers are orthotropic. Therefore, the stress–strain relations in kth layer, in principal material coordinates, are obtained from the following:

$$\begin{Bmatrix} \sigma_1 \\ \sigma_2 \\ \tau_{12} \end{Bmatrix}^{(k)} = \begin{bmatrix} Q_{11} & Q_{12} & 0 \\ Q_{12} & Q_{22} & 0 \\ 0 & 0 & Q_{66} \end{bmatrix}^{(k)} \begin{Bmatrix} \varepsilon_1 \\ \varepsilon_2 \\ \gamma_{12} \end{Bmatrix}^{(k)} \tag{6}$$

where the subscripts 1 and 2 refer to the material coordinate system (x_1, x_2). The material coordinate axis x_1 is taken to be the direction of the fiber and the x_2-axis is perpendicular to fiber longitudinal direction (see Fig. 1). The plane stress–reduced stiffnesses Q_{ij} are:

$$Q_{11} = \frac{E_1}{1-\upsilon_{12}\upsilon_{21}}\ ,\ Q_{22} = \frac{E_2}{1-\upsilon_{12}\upsilon_{21}}\ ,\ Q_{12} = \frac{\upsilon_{12}E_2}{1-\upsilon_{12}\upsilon_{21}}\ \ ,\ \ Q_{66} = G_{12} \tag{7}$$

where E_1 and E_2 are the moduli of elasticity in 1 and 2 directions, G_{12} is the shear modulus, and υ_{12} is the major Poisson ratio. In Eq. (6), stress-strain relations are expressed in principal material coordinates, but a laminated composite is made of several orthotropic layers and each layer has its own principal material coordinates. Therefore, the stresses and strains must be transformed to the local coordinates X and Y. For that purpose, the following transformation matrices are used:

$$\begin{Bmatrix}\sigma_1\\ \sigma_2\\ \tau_{12}\end{Bmatrix}=\begin{bmatrix}\cos^2\theta(X) & \sin^2\theta(X) & 2\sin\theta(X)\cos\theta(X)\\ \sin^2\theta(X) & \cos^2\theta(X) & -2\sin\theta(X)\cos\theta(X)\\ -\sin\theta(X)\cos\theta(X) & \sin\theta(X)\cos\theta(X) & -\sin^2\theta(X)+\cos^2\theta(X)\end{bmatrix}\begin{Bmatrix}\sigma_X\\ \sigma_Y\\ \tau_{XY}\end{Bmatrix} \tag{8}$$

$$\begin{Bmatrix}\varepsilon_1\\ \varepsilon_2\\ \gamma_{12}\end{Bmatrix}=\begin{bmatrix}\cos^2\theta(X) & \sin^2\theta(X) & \sin\theta(X)\cos\theta(X)\\ \sin^2\theta(X) & \cos^2\theta(X) & -\sin\theta(X)\cos\theta(X)\\ -2\sin\theta(X)\cos\theta(X) & 2\sin\theta(X)\cos\theta(X) & -\sin^2\theta(X)+\cos^2\theta(X)\end{bmatrix}\begin{Bmatrix}\varepsilon_X\\ \varepsilon_Y\\ \gamma_{XY}\end{Bmatrix} \tag{9}$$

where θ is the fiber angle in Eq. (1) and can be different at any point of a layer of VSCL plate. The stress–strain relations in the local coordinate system are presented as [5]:

$$\begin{Bmatrix}\sigma_X(X,Y,Z,t)\\ \sigma_Y(X,Y,Z,t)\\ \tau_{XY}(X,Y,Z,t)\end{Bmatrix}^{(k)}=\begin{bmatrix}\bar{Q}_{11}(X) & \bar{Q}_{12}(X) & \bar{Q}_{16}(X)\\ \bar{Q}_{12}(X) & \bar{Q}_{22}(X) & \bar{Q}_{26}(X)\\ \bar{Q}_{16}(X) & \bar{Q}_{26}(X) & \bar{Q}_{66}(X)\end{bmatrix}^{(k)}\begin{Bmatrix}\varepsilon_X(X,Y,Z,t)\\ \varepsilon_Y(X,Y,Z,t)\\ \gamma_{XY}(X,Y,Z,t)\end{Bmatrix}^{(k)} \tag{10}$$

In Eq. (10), the transformed reduced stiffnesses $\bar{Q}_{ij}(X)$ are functions of coordinates X. Therefore, they are not constant over the laminate and are given by [5]:

$$\begin{aligned}
\bar{Q}_{11}(\theta(X)) &= Q_{11}\cos^4\theta(X)+2(Q_{12}+2Q_{66})\sin^2\theta(X)\cos^2\theta(X)+Q_{22}\sin^4\theta(X)\\
\bar{Q}_{12}(\theta(X)) &= (Q_{11}+Q_{22}-4Q_{66})\sin^2\theta(X)\cos^2\theta(X)+Q_{12}(\sin^4\theta(X)+\cos^4\theta(X))\\
\bar{Q}_{22}(\theta(X)) &= Q_{11}\sin^4\theta(X)+2(Q_{12}+2Q_{66})\sin^2\theta(X)\cos^2\theta(X)+Q_{22}\cos^4\theta(X)\\
\bar{Q}_{16}(\theta(X)) &= (Q_{11}-Q_{12}-2Q_{66})\sin\theta(X)\cos^3\theta(X)+(Q_{12}-Q_{22}+2Q_{66})\sin^3\theta(X)\cos\theta(X)\\
\bar{Q}_{26}(\theta(X)) &= (Q_{11}-Q_{12}-2Q_{66})\sin^3\theta(X)\cos\theta(X)+(Q_{12}-Q_{22}+2Q_{66})\sin\theta(X)\cos^3\theta(X)\\
\bar{Q}_{66}(\theta(X)) &= (Q_{11}+Q_{22}-2Q_{12}-2Q_{66})\sin^2\theta(X)\cos^2\theta(X)+Q_{66}(\sin^4\theta(X)+\cos^4\theta(X))
\end{aligned} \tag{11}$$

The in-plane force resultants per unit length are given by:

$$\begin{Bmatrix}N_{XX}\\ N_{YY}\\ N_{XY}\end{Bmatrix}=\sum_{k=1}^{n}\int_{Z_k}^{Z_{k+1}}\begin{Bmatrix}\sigma_{XX}\\ \sigma_{YY}\\ \tau_{XY}\end{Bmatrix}dZ=\begin{bmatrix}A_{11}(X) & A_{12}(X) & A_{16}(X)\\ A_{12}(X) & A_{22}(X) & A_{26}(X)\\ A_{16}(X) & A_{26}(X) & A_{66}(X)\end{bmatrix}\begin{Bmatrix}\varepsilon^{(0)}{}_{XX}\\ \varepsilon^{(0)}{}_{YY}\\ \gamma^{(0)}{}_{XY}\end{Bmatrix}+\begin{bmatrix}B_{11}(X) & B_{12}(X) & B_{16}(X)\\ B_{12}(X) & B_{22}(X) & B_{26}(X)\\ B_{16}(X) & B_{26}(X) & B_{66}(X)\end{bmatrix}\begin{Bmatrix}\varepsilon^{(1)}{}_{XX}\\ \varepsilon^{(1)}{}_{YY}\\ \gamma^{(1)}{}_{XY}\end{Bmatrix} \tag{12}$$

The moment resultants per unit length are given by:

$$\begin{Bmatrix}M_{XX}\\ M_{YY}\\ M_{XY}\end{Bmatrix}=\sum_{k=1}^{n}\int_{Z_k}^{Z_{k+1}}\begin{Bmatrix}\sigma_{XX}\\ \sigma_{YY}\\ \tau_{XY}\end{Bmatrix}ZdZ=\begin{bmatrix}B_{11}(X) & B_{12}(X) & B_{16}(X)\\ B_{12}(X) & B_{22}(X) & B_{26}(X)\\ B_{16}(X) & B_{26}(X) & B_{66}(X)\end{bmatrix}\begin{Bmatrix}\varepsilon^{(0)}{}_{XX}\\ \varepsilon^{(0)}{}_{YY}\\ \gamma^{(0)}{}_{XY}\end{Bmatrix}+\begin{bmatrix}D_{11}(X) & D_{12}(X) & D_{16}(X)\\ D_{12}(X) & D_{22}(X) & D_{26}(X)\\ D_{16}(X) & D_{26}(X) & D_{66}(X)\end{bmatrix}\begin{Bmatrix}\varepsilon^{(1)}{}_{XX}\\ \varepsilon^{(1)}{}_{YY}\\ \gamma^{(1)}{}_{XY}\end{Bmatrix} \tag{13}$$

where A_{ij}, D_{ij}, and B_{ij} are called extensional stiffnesses, bending stiffnesses, and bending- extensional coupling stiffnesses, respectively. When the laminates are symmetric about their middle plane, there is no linear coupling between the membrane deformations and bending [3]. In this article, VSCL plates symmetric about their middle plane will be analyzed and, therefore, B_{ij} are null. A_{ij} and D_{ij} are defined in terms of $\bar{Q}_{ij}$ as:

$$A_{ij}(X), D_{ij}(X) = \int_{-h/2}^{h/2} \bar{Q}_{ij}^{(k)}(1, Z^2)dZ = \sum_{k=1}^{n} \int_{Z_k}^{Z_{k+1}} \bar{Q}_{ij}^{(k)}(1, Z^2)dZ \tag{14}$$

or

$$\begin{aligned} A_{ij}(X) &= \sum_{k=1}^{n} \bar{Q}_{ij}^{(k)}(Z_{k+1} - Z_k) \\ D_{ij}(X) &= \frac{1}{3}\sum_{k=1}^{n} \bar{Q}_{ij}^{(k)}(Z_{k+1}^3 - Z_k^3) \end{aligned} \tag{15}$$

2.2 Finite strip method for free vibration analysis of VSCL flat plates

In the finite strip method (FSM), the plate is divided into a finite number of strips that are connected along the so-called nodal lines. Displacements and rotations represent the degrees of freedom of each nodal line (Fig. 3).

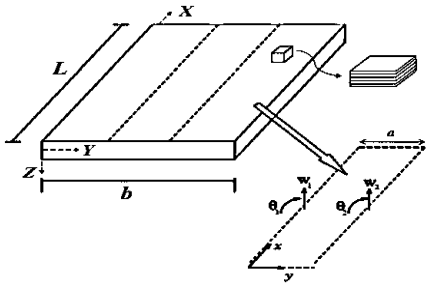

Fig.3
A plate which is divided to some finite strips.

The transverse displacement of the strip is approximated as a combination of the trigonometric series in the longitudinal direction x and the polynomial function $f(y)$ in the lateral direction y. Thus the transverse displacement function for each strip is chosen in the form [10]:

$$w = \sum_{n=1}^{r} S_n(x)\{f(y)\}\{d_n(t)\} \tag{16}$$

where the vector of nodal line displacements for the nth harmonic $d_n(t)$ is given by:

$$\{d_n(t)\} = \{\theta_{1n}, w_{1n}, \theta_{2n}, w_{2n}\}^T \tag{17}$$

and $f(y)$ for a strip with the width a is defined as follows [10]:

$$\{f(y)\} = \left\{\left(y - 2\frac{y^2}{a} + \frac{y^3}{a^2}\right), \left(1 - 3\frac{y^2}{a^2} + 2\frac{y^3}{a^3}\right), \left(-\frac{y^2}{a} + \frac{y^3}{a^2}\right), \left(3\frac{y^2}{a^2} - 2\frac{y^3}{a^3}\right)\right\} \tag{18}$$

The following basic function series $S_n(x)$ corresponding to different types of end conditions in $x = 0$ and $x = L$ can be used in FSM [11]:

a. Both simply supported. Using boundary condition $S_n(0) = S_n''(0) = S_n(L) = S_n''(L) = 0$, the specific forms of S_n become

$$S_n(x) = \sin\frac{\mu_n}{L}x; \quad (\mu_n = \pi, 2\pi, 3\pi, ..., n\pi)$$

b. Both clamped. Using boundary condition $S_n(0)=S_n'(0)=S_n(L)=S_n'(L)=0$, the specific forms of S_n become

$$S_n(x)=\sin\frac{\mu_n}{L}x\times\sin\frac{\pi}{L}x;\quad(\mu_n=\pi,2\pi,3\pi,...,n\pi)$$

c. Clamped at $x = 0$ and free edge at $x = L$. Using boundary condition $S_n(0)=S_n'(0)=S_n''(L)=S_n'''(L)=0$, the specific forms of S_n become

$$S_n(x)=1-\cos\frac{\mu_n}{L}x;\quad(\mu_n=\frac{\pi}{2},\frac{3\pi}{2},\frac{5\pi}{2},...,(n-\frac{1}{2})\pi)$$

In order to obtain stiffness matrix and mass matrix, the energy method is adopted. The bending strain energy U_b for each strip can be written as:

$$U_b=\frac{1}{2}\int_A\{M\}^T\{\varepsilon^1\}dA=\frac{1}{2}\int_A\begin{Bmatrix}M_{xx} & M_{yy} & M_{xy}\end{Bmatrix}\begin{Bmatrix}\varepsilon_{xx}^{(1)}\\ \varepsilon_{yy}^{(1)}\\ \gamma_{xy}^{(1)}\end{Bmatrix}dA \tag{19}$$

By using Eq. (5) and Eq. (13), and assuming B_{ij}=0 (the equations mentioned in Section 2.1, can be used in the *xyz* coordinates system), the bending strain energy U_b can be rewritten as:

$$U_b=\frac{1}{2}\int_A\left[D_{11}\left(\frac{\partial^2w}{\partial x^2}\right)^2+D_{22}\left(\frac{\partial^2w}{\partial y^2}\right)^2+2D_{12}\frac{\partial^2w}{\partial x^2}\frac{\partial^2w}{\partial y^2}+4D_{66}\left(\frac{\partial^2w}{\partial x\,\partial y}\right)^2+4D_{16}\frac{\partial^2w}{\partial x^2}\frac{\partial^2w}{\partial x\,\partial y}+4D_{26}\frac{\partial^2w}{\partial y^2}\frac{\partial^2w}{\partial x\,\partial y}\right]dA \tag{20}$$

and by replacement the displacement field of a strip from Eq. (16), it can be obtained as:

$$U_b=\frac{1}{2}\sum_{m=1}^{r}\sum_{n=1}^{r}\{d_m\}^T[k_b]_{mn}\{d_n\} \tag{21}$$

where $[k_b]$ is the bending stiffness matrix of the strip and can be obtained as:

$$[k_b]_{mn}=\int_A[B_b]_m^T[D][B_b]_n\,dA \tag{22}$$

where $[B_b]_n$ and $[D]$ are defined as:

$$[B_b]_n=\begin{bmatrix}\frac{\partial^2(f_{11}S_n)}{\partial x^2} & \frac{\partial^2(f_{12}S_n)}{\partial x^2} & \frac{\partial^2(f_{13}S_n)}{\partial x^2} & \frac{\partial^2(f_{14}S_n)}{\partial x^2}\\ \frac{\partial^2(f_{11}S_n)}{\partial y^2} & \frac{\partial^2(f_{12}S_n)}{\partial y^2} & \frac{\partial^2(f_{13}S_n)}{\partial y^2} & \frac{\partial^2(f_{14}S_n)}{\partial y^2}\\ 2\frac{\partial^2(f_{11}S_n)}{\partial x\,\partial y} & 2\frac{\partial^2(f_{12}S_n)}{\partial x\,\partial y} & 2\frac{\partial^2(f_{13}S_n)}{\partial x\,\partial y} & 2\frac{\partial^2(f_{14}S_n)}{\partial x\,\partial y}\end{bmatrix} \tag{23}$$

$$[D]=\begin{bmatrix}D_{11} & D_{12} & D_{16}\\ D_{12} & D_{22} & D_{26}\\ D_{16} & D_{26} & D_{66}\end{bmatrix} \tag{24}$$

The kinetic energy for each strip T with the density ρ is [10]:

$$T = \frac{1}{2}\int_{st} \rho h \left(\frac{\partial w}{\partial t}\right)^2 dA \tag{25}$$

That

$$\begin{aligned} &\delta \int_{t_i}^{t_f} T dt = \int_{t_i}^{t_f}\int_{A} \rho h \left(\frac{\partial \delta w}{\partial t}\right)\left(\frac{\partial w}{\partial t}\right) dA\, dt = \int_{A} \rho h \left(\delta w\right)\left(\frac{\partial w}{\partial t}\right) dA \Bigg|_{t_i}^{t_f} - \int_{t_i}^{t_f}\int_{A} \rho h \left(\delta w\right)\left(\frac{\partial^2 w}{\partial t^2}\right) dA\, dt \\ &\Rightarrow \delta \int_{t_i}^{t_f} T dt = -\int_{t_i}^{t_f} \sum_{m=1}^{r}\sum_{n=1}^{r} \{\delta d_m\}^T \left[m_b\right]_{mn} \left\{\ddot{d}_n\right\} dt \end{aligned} \tag{26}$$

where $[m_b]$ is the mass matrix and can be obtained by

$$\left[m_b\right]_{mn} = \int_{A} \rho h \left\{f\left(y\right)\right\}^T \left\{f\left(y\right)\right\} S_m S_n dA \tag{27}$$

The stiffness matrix of the flat plate [K] and the mass matrix of the flat plate [M] can be obtained by common methods of assembling [k_b] and [m_b] matrices of all strips of plate. Finally, free vibration frequencies of flat plate ω can be obtained by solving the following equation

$$\left|\left[K\right] - \omega^2 \left[M\right]\right| = 0 \tag{28}$$

2.3 Finite strip method for free vibration analysis of VSCL folded plates

VSCL folded plates can be considered as a compound of rectangular VSCL flat plates, which are simultaneously subjected to bending and in-plane action. Then at each of the two nodal lines there are four displacement components u, v, θ, and w (Fig. 4).

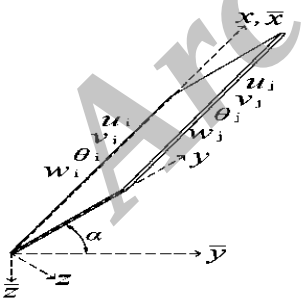

Fig.4
Local and global coordinates and displacement components in the local coordinates.

The approximation of displacements u and v in a single strip has the form [12]

$$\begin{Bmatrix} u \\ v \end{Bmatrix} = \sum_{n=1}^{r} \begin{bmatrix} (1-\frac{y}{a})(\frac{L}{\mu_n})S_n' & 0 & (\frac{y}{a})(\frac{L}{\mu_n})S_n' & 0 \\ 0 & (1-\frac{y}{a})S_n & 0 & (\frac{y}{a})S_n \end{bmatrix} \{\delta\}_n = \sum_{n=1}^{r} [C]_n \{\delta\}_n \tag{29}$$

where the vector of degrees of freedom corresponding to the nth harmonic $\delta_n(t)$ is given by

$$\{\delta_n(t)\} = \{u_{1n}, v_{1n}, u_{2n}, v_{2n}\}^T \tag{30}$$

The energy due to in-plane forces U_g for each strip can be written as:

$$U_g = \frac{1}{2}\int_A \{N\}^T \{\varepsilon^0\} dA = \frac{1}{2}\int_A \{N_{xx} \quad N_{yy} \quad N_{xy}\} \begin{Bmatrix} \varepsilon_{xx}^{(0)} \\ \varepsilon_{yy}^{(0)} \\ \gamma_{xy}^{(0)} \end{Bmatrix} dA \tag{31}$$

By using Eq. (4), Eq. (12), and Eq. (29), and assuming B_{ij}=0 and w_0=0, the energy due to in-plane forces U_g can be obtained as:

$$U_g = \frac{1}{2}\sum_{m=1}^{r}\sum_{n=1}^{r} \{\delta_m\}^T [k_p]_{mn} \{\delta_n\} \tag{32}$$

where $[k_p]$ is the in-plane stiffness matrix of the strip and can be obtained as:

$$[k_p]_{mn} = \int_A [B_p]_m^T [A][B_p]_n \, dA \tag{33}$$

where $[B_p]_n$ and $[A]$ are defined as:

$$[B_p]_n = \begin{bmatrix} \left(1-\frac{y}{a}\right)\left(\frac{L}{\mu_n}\right)S_n'' & 0 & \left(\frac{y}{a}\right)\left(\frac{L}{\mu_n}\right)S_n'' & 0 \\ 0 & -\frac{1}{a}S_n & 0 & \frac{1}{a}S_n \\ \left(\frac{-1}{a}\right)\left(\frac{L}{\mu_n}\right)S_n' & \left(1-\frac{y}{a}\right)S_n' & \left(\frac{1}{a}\right)\left(\frac{L}{\mu_n}\right)S_n' & \left(\frac{y}{a}\right)S_n' \end{bmatrix} \tag{34}$$

$$[A] = \begin{bmatrix} A_{11} & A_{12} & A_{16} \\ A_{12} & A_{22} & A_{26} \\ A_{16} & A_{26} & A_{66} \end{bmatrix} \tag{35}$$

Also, the in-plane mass matrix of the strip $[m_p]$ can be obtained as:

$$[m_p]_{mn} = \rho h \int_A [C]_m^T [C]_n \, dA \tag{36}$$

where $[C]$ denotes the shape function defined in Eq. 29.

The stiffness and mass matrix of such a strip can be obtained as an appropriate assembly of stiffness and mass matrices for strips in the bending state and in-plane state as follows:

$$[k]_{mn} = \begin{bmatrix} [k_p]_{mn} & 0 \\ 0 & [k_b]_{mn} \end{bmatrix}_{mn} \tag{37}$$

$$[m]_{mn} = \begin{bmatrix} [m_p]_{mn} & 0 \\ 0 & [m_b]_{mn} \end{bmatrix}_{mn} \tag{38}$$

These matrices correspond to the following vector of degrees of freedom

$$\{\psi_n(t)\} = \{u_{1n}, v_{1n}, u_{2n}, v_{2n}, \theta_{1n}, w_{1n}, \theta_{2n}, w_{2n}\}^T \tag{39}$$

The stiffness and mass matrix of the strip should be transferred from local coordinates to the global one. In Fig. 4, the local coordinates are labelled as x, y, z and the global coordinates are labelled as $\bar{x}, \bar{y}, \bar{z}$ .The transformations of mass and stiffness matrix of the strip between the two sets of coordinate systems are given by

$$[\bar{k}]_{mn} = [T]^T [k]_{mn} [T] \tag{40}$$

$$[\bar{m}]_{mn} = [T]^T [m]_{mn} [T] \tag{41}$$

where $[\bar{k}]$ and $[\bar{m}]$ are the stiffness and mass matrix in the global coordinates, respectively, and $[T]$ is the transformation matrix as:

$$T = \begin{bmatrix} 1 & 0 & 0 & 0 & 0 & 0 & 0 & 0 \\ 0 & \cos\alpha & 0 & 0 & 0 & \sin\alpha & 0 & 0 \\ 0 & 0 & 1 & 0 & 0 & 0 & 0 & 0 \\ 0 & 0 & 0 & \cos\alpha & 0 & 0 & 0 & \sin\alpha \\ 0 & 0 & 0 & 0 & 1 & 0 & 0 & 0 \\ 0 & -\sin\alpha & 0 & 0 & 0 & \cos\alpha & 0 & 0 \\ 0 & 0 & 0 & 0 & 0 & 0 & 1 & 0 \\ 0 & 0 & 0 & -\sin\alpha & 0 & 0 & 0 & \cos\alpha \end{bmatrix} \tag{42}$$

where α is the angle between the y and $\bar{y}$ axes. The stiffness matrix of the folded plate $[K']$ and the mass matrix of the folded plate $[M']$ can be obtained by common methods of assembling $[\bar{k}]$ and $[\bar{m}]$ matrices of all strips of plate and writing these matrices in the form of reduced matrices (by satisfying the boundary conditions at the straight lines). Finally, free vibration frequencies of folded plate ω can be obtained by solving the following equation:

$$\left|[K'] - [M']\omega^2\right| = 0 \tag{43}$$

3 NUMERICAL RESULTS

This section is divided into two parts. First, the accuracy of the present FSM is investigated by comparing the result of free vibration analysis results of CSCL and VSCL flat plates, isotropic folded plates, and CSCL folded plates with the findings of previous studies (there is no data in the field of VSCL folded plates analysis). Secondly, free vibration analysis of VSCL flat plates and VSCL folded plates is studied. The properties of the plates analyzed are defined in Table 1. The folded plates that are investigated in this article are one-fold, two-fold, three-fold, and four-fold folded plates (Fig. 5). The parameters n and NS represent the number of terms of basic functions and the number of finite strips with equal width, respectively. In addition, in the flat plates, two types of boundary

conditions as four edges clamped CCCC and four edges simply supported SSSS are studied, and in the folded plates, four type of boundary conditions as SSSS, SFSF, SCSC, SCSF are studied, as defined below.

SSSS: At $x = 0$ and $x = L$, simply supported. At straight lines, simply supported.

SFSF: At $x = 0$ and $x = L$, simply supported. At straight lines, free.

SCSC: At $x = 0$ and $x = L$, simply supported. At straight lines, clamped.

SCSF: At $x = 0$ and $x = L$, simply supported. At straight lines, clamped and free.

Table 1
Mechanical properties of the plates.

	E_1(Gpa)	E_2(Gpa)	G_{12}(Gpa)	ν_{12}	ρ (kg/m^3)
Plate 1, Ref. [14] for E_1=173 Gpa	173	70.612	33.89	0.23	8000
Plate 2, Ref. [1]	173	7.2	3.76	0.29	1540
Plate 3, Ref. [20]	60.7	24.8	12	0.23	1300
Plate 4, Ref. [21] for E_1=257.5 Gpa	257.5	10.3	5.15	0.25	1600

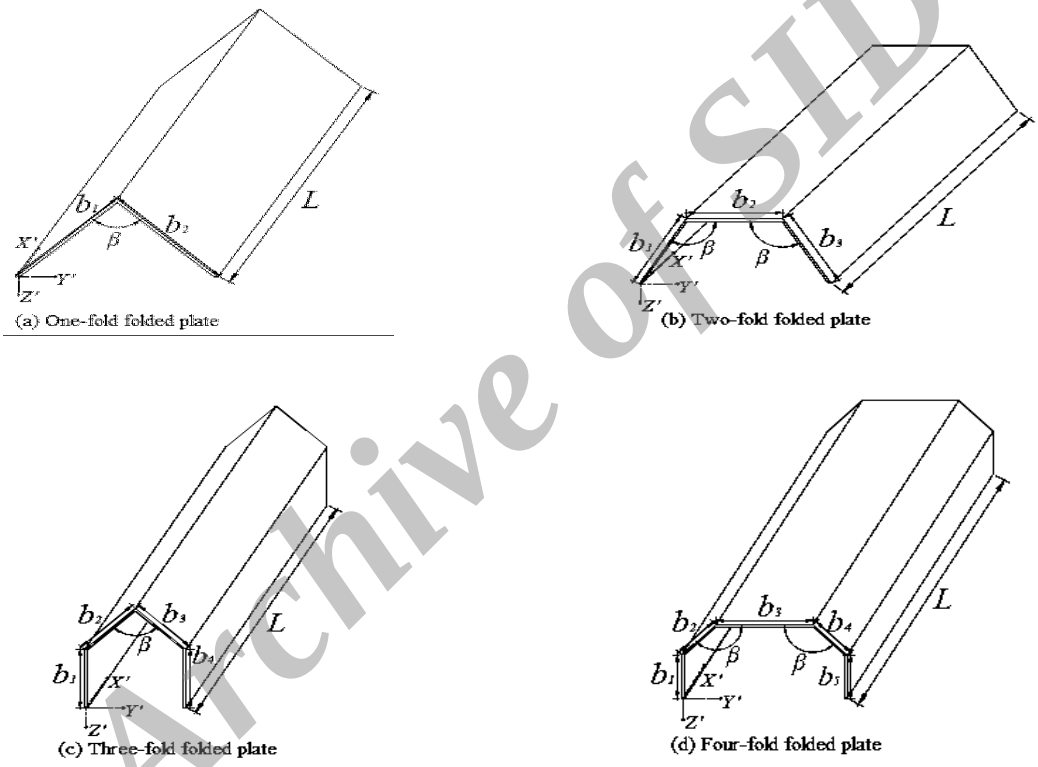

Fig.5
Geometrical properties of the folded plates.

3.1 Validation

In Table 2. and Table 3., the results of free vibration analysis of three-layer CSCL flat plates obtained by the present FSM are compared with those of relevant studies [13,14,15,16]. In this comparison, the normalized natural frequency is determined as $\varpi = \omega L^2 \sqrt{12\rho(1-\upsilon_{12}\upsilon_{21})/E_1 h^2}$. The mechanical properties are the same as those of Plate 1 in Table 1., and the geometry is L=1m, b=1m, and h=0.06m. The results presented in Table 2. and Table 3. represent the frequencies of the CSCL plates for SSSS and CCCC boundary conditions, respectively. In Table 3., analysis has been performed with different values of n. Here, by using n=6, we come close to the a suitable response.

In Table 4., the results of free vibration analysis of four-layer VSCL flat plates obtained by the present FSM are compared with those of Houmat [5]. In this comparison, the normalized natural frequency is determined

as $\varpi = \omega L\sqrt{\rho / E_2}$. The mechanical properties are the same as those of Plate 2 in Table 1., and the geometry is L=0.5m, b=0.5m, and h=0.005m. The boundary conditions are considered CCCC, and the stacking sequence is $[\mp\langle T_0/T_1\rangle]_S$ which means $[+\langle T_0/T_1\rangle, -\langle T_0/T_1\rangle, -\langle T_0/T_1\rangle, +\langle T_0/T_1\rangle]$. In addition, in this table, analysis has been performed with different values of n. Here, by using n=9, we come close to the suitable response.

Natural frequencies of a cantilever isotropic one-fold folded plate (as shown in Fig. 5(a)) are presented in Table 5. The plate is clamped at $X' = 0$ and its geometric properties are as follows: β =150°, b_1=b_2=0.5L and h=0.02L. The Young's modulus E is taken to be 10.92 Gpa, the Poisson's ratio υ is 0.3 and the density ρ is 1000 kg/m^3. In the table, the first three normalized frequencies of the plate obtained by the present FSM are compared with those of relevant studies [17,18,19]. In this comparison, the normalized natural frequency is determined as $\varpi = \omega L\sqrt{\rho(1-\upsilon^2)/E}$.

Fundamental frequencies of a cantilever CSCL two-fold folded plate (as seen in Fig. 5(b)) with clamped boundary condition at $X' = 0$ are shown in Table 6. The geometric properties of the plate are as follows: b_1=b_2=b_3=L/3, h=0.02L. The mechanical properties are the same as those of Plate 3 in Table 1. and the stacking sequence is [30/-30/-30/30]. In the table, the results obtained by the present FSM are compared with those of relevant studies [19,20,21]. In this comparison, the normalized natural frequency is determined as $\varpi = \omega L\sqrt{\rho(1-\upsilon_{12}{}^2)/E_1}$.

In Table 7. , the first four normalized frequencies of CSCL four-fold folded plate obtained by the present FSM are compared with those obtained by Haldar and Sheikh [22]. In this comparison, the normalized natural frequency is determined as $\varpi = \omega L^2\sqrt{\rho / E_2 h^2}$. The mechanical properties are the same as those of Plate 4 in Table 1. The geometry corresponds to Fig.5(d) (b_1=b_2=b_4=b_5=L/6, b_3=L/3, h=0.01L and the crank angle β is considered as being various). The boundary conditions are considered SFSF, and the stacking sequence is [90/0/90].

As shown in all the tables (i.e., Tables 2-7), the results obtained by the present FSM agree well with those obtained in similar studies.

Table 2
Normalized natural frequencies of fully simply supported CSCL flat plates.

		Mode					
stacking sequence		1	2	3	4	5	6
[0/0/0]	Present: FSM [NS=4, n=3]	15.171	33.253	44.387	60.678	64.521	90.192
	Exact-CLPT Ref. [13]	15.171	33.248	44.387	60.682	64.457	90.145
	CLPT Ref. [14]	15.19	33.31	44.52	60.79	64.55	90.31
	CLPT Ref. [15]	15.19	33.30	44.42	60.78	64.53	90.29
[15/-15/15]	Present: FSM [NS=4, n=3]	15.530	34.395	43.949	62.124	66.29	91.544
	CLPT Ref. [14]	15.37	34.03	43.93	60.80	66.56	91.40
	CLPT Ref. [15]	15.43	34.09	43.80	60.85	66.67	91.40
[30/-30/30]	Present: FSM [NS=4, n=3]	16.226	37.148	42.567	64.907	71.311	85.916
	CLPT Ref. [14]	15.86	35.77	42.48	61.27	71.41	85.67
	CLPT Ref. [15]	15.90	35.86	42.62	61.45	71.71	85.72

Table 3
The normalized fundamental frequency of fully clamped CSCL flat plate.

	Present FSM [NS=4]							
stacking sequence	n=1	n=2	n=3	n=4	n=5	n=6	Ref. [14]	Ref. [16]
[45/-45/45]	29.39	28.88	28.58	28.51	28.45	28.41	28.38	28.50
[30/-30/30]	29.46	29.06	28.74	28.68	28.62	28.60	28.55	28.69
[15/-15/15]	29.56	29.42	29.06	29.04	28.97	29.94	28.92	29.07
[0/0/0]	29.61	29.61	29.22	29.22	29.15	29.15	29.13	29.27

Table 4
The normalized fundamental frequency of fully clamped VSCL flat plate.

	Present FSM [NS=6]									
stacking sequence	n=1	n=2	n=3	n=4	n=5	n=6	n=7	n=8	n=9	Ref. [5]
$[\mp\langle 40/80\rangle]_s$	0.308	0.288	0.277	0.273	0.273	0.270	0.269	0.268	0.268	0.268
$[\mp\langle 40/70\rangle]_s$	0.311	0.289	0.281	0.276	0.274	0.273	0.272	0.272	0.271	0.270
$[\mp\langle 40/60\rangle]_s$	0.315	0.292	0.286	0.281	0.280	0.279	0.278	0.278	0.278	0.276
$[\mp\langle 40/50\rangle]_s$	0.320	0.297	0.293	0.289	0.287	0.286	0.285	0.285	0.285	0.284
$[\mp\langle 40/30\rangle]_s$	0.335	0.312	0.310	0.308	0.308	0.308	0.307	0.307	0.307	0.306
$[\mp\langle 40/20\rangle]_s$	0.341	0.319	0.318	0.317	0.317	0.316	0.316	0.316	0.315	0.315
$[\mp\langle 40/10\rangle]_s$	0.345	0.325	0.324	0.324	0.323	0.323	0.323	0.323	0.322	0.322

Table 5
The first three normalized frequencies of cantilever isotropic one-fold folded plate (clamped at x=0).

	Mode		
	1	2	3
Present FSM [NS=4, n=4]	0.0491	0.0805	0.1792
Ref. [17]	0.0490	0.0801	0.1778
Ref. [18]	0.0489	0.0801	0.1778
Ref. [18]	0.0491	0.0804	0.1883

Table 6
The normalized fundamental frequency of cantilever CSCL two-fold folded plate (clamped at x=0).

Crank angle	Present FSM [NS=6, n=4]	Ref. [20]	Ref. [19]	Ref. [21]
β =90°	0.0922	0.0921	0.0901	0.0925
β =120°	0.0816	0.0800	0.0781	0.0736
β =150°	0.570	0.0573	0.0551	0.0522

Table 7
The first four normalized frequencies of CSCL four-fold folded plate (simply supported at x=0, L and other two sides being free).

		Mode			
Crank angle		1	2	3	4
β =150°	Present FSM [NS=12, n=3]	46.369	67.548	83.409	90.807
	Ref. [22]	46.215	67.151	84.321	90.213
β =135°	Present FSM [NS=12, n=3]	44.720	58.366	83.387	88.108
	Ref. [22]	44.814	58.331	84.029	87.038
β =120°	Present FSM [NS=12, n=3]	38.786	49.311	71.549	75.661
	Ref. [22]	38.575	49.126	72.362	76.231

3.2 Free vibration analysis
3.2.1 Variable stiffness composite laminated flat plate

In this study, we conducted the free vibration analysis of a three-layer VSCL flat plate. The mechanical properties are the same as those of Plate 2 in Table 1. The geometry is L=0.5m, b=0.5m and h=0.005m. In addition, the

stacking sequence is considered as $[+\langle T_0/T_1\rangle, -\langle T_0/T_1\rangle, +\langle T_0/T\rangle_1]$. The results of this analysis are determined as the normalized natural frequency $\varpi = \omega L\sqrt{\rho/E_2}$, as shown in Table 8. and Table 9.

In Table 8. , the first six normalized frequencies of this plate with SSSS boundary conditions are presented. Also, the same results appear in Fig. 6. As seen, when the value of T_1 is increased while keeping constant the value of T_0, the first natural frequencies increase. Also, when the value of T_1 remains constant, the first natural frequencies increase as the value of T_0 varies from 0° to 30°. Nonetheless, by performing free vibration analysis of VSCL flat plate, but with CCCC boundary conditions, Yazdani and Ribeiro [8] realized that by increasing T_1 and keeping T_0 constant, the first natural frequencies decrease.

In Table 9., the normalized fundamental frequency of this plate with CCCC boundary conditions is presented. In this table, it could be seen that by increasing either T_0 or T_1, and keeping another constant, normalized fundamental frequency decreases.

Table 8
The first six normalized frequencies of fully simply supported VSCL flat plate (NS=4, *n*=4).

		Mode					
T_0	T_1	1	2	3	4	5	6
0°	0°	0.150	0.203	0.328	0.558	0.568	0.601
	10°	0.154	0.215	0.345	0.568	0.577	0.612
	20°	0.164	0.246	0.390	0.566	0.628	0.640
	30°	0.176	0.282	0.445	0.560	0.674	0.698
	40°	0.186	0.314	0.498	0.550	0.703	0.773
10°	0°	0.151	0.211	0.340	0.568	0.574	0.612
	10°	0.157	0.231	0.371	0.564	0.610	0.629
	20°	0.168	0.266	0.425	0.560	0.661	0.676
	30°	0.180	0.304	0.485	0.550	0.697	0.758
	40°	0.191	0.336	0.537	0.541	0.725	0.844
20°	0°	0.154	0.232	0.381	0.566	0.633	0.640
	10°	0.161	0.256	0.422	0.560	0.661	0.688
	20°	0.173	0.296	0.481	0.551	0.694	0.768
	30°	0.185	0.333	0.539	0.544	0.729	0.861
	40°	0.195	0.364	0.523	0.602	0.756	0.957
30°	0°	0.157	0.266	0.451	0.560	0.674	0.756
	10°	0.166	0.296	0.500	0.550	0.697	0.826
	20°	0179	0.333	0.539	0.562	0.729	0.917
	30°	0.190	0.369	0.526	0.626	0.762	1.019
	40°	0.198	0.398	0.508	0.684	0.785	1.004

Table 9
The normalized fundamental frequency of fully clamped VSCL flat plate (NS=4, *n*=8).

$\langle T_0,T_1\rangle$	$\langle 0/10\rangle$	$\langle 0/20\rangle$	$\langle 0/30\rangle$	$\langle 0/40\rangle$	$\langle 10/0\rangle$	$\langle 20/0\rangle$	$\langle 30/0\rangle$	$\langle 40/0\rangle$
ϖ	0.324	0.314	0.299	0.282	0.326	0.321	0.316	0.311

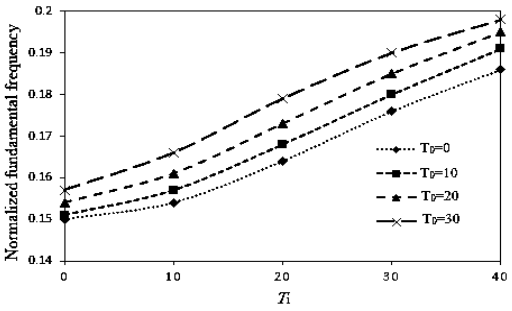

Fig.6
The effect of T_0 and T_1 on the normalized fundamental frequency of VSCL plate, simply supported at all edges.

3.2.2 Variable stiffness composite laminated folded plates

In this section, we study the free vibration analysis of VSCL one-fold, two-fold, three-fold and four-fold folded plates and the normalized natural frequency is determined as $\varpi = \omega L\sqrt{\rho / E_2}$. In Table 10. and Table 11. , the mechanical properties of the plates investigated are the same as those of Plate 2 in Table 1. The geometry of these plates is shown in Fig.5 and their dimensions are listed as follows:

For one-fold folded plate: $b_1= b_2=L/2$ and $h=0.01L$.

For two-fold folded plate: $b_1= b_2= b_3=L/3$ and $h=0.01L$.

For three-fold folded plate: $b_1= b_2= b_3= b_4=L/4$ and $h=0.01L$.

For four-fold folded plate: $b_1= b_2= b_4= b_5=L/6$, $b_3=L/3$ and $h=0.01L$.

In Table 10., the first four normalized frequencies of VSCL one-fold and two-fold folded plates with three types of stacking sequence are presented. The boundary conditions are considered SFSF, and the crank angle is assumed $\beta=120°$.

In Table 11., the effect of crank angle β on the natural frequencies of VSCL one-fold, two-fold, three-fold and four-fold folded plates is investigated. The boundary conditions of all these folded plates are considered SFSF, and the stacking sequence is $[\langle 0/45\rangle,\langle -45/-60\rangle,\langle 0/45\rangle]$. As seen, when the folding order is increased from one-folding to four folding, by changing the crank angle, more variation is created in the natural frequencies. In other words, the crank angle has no significant effect on the natural frequencies for VSCL one-fold folded plate whereas it has significant effects on the natural frequencies for VSCL four-fold folded plate.

In Table 12. , the first four normalized frequencies of VSCL four-fold folded plate are determined. The geometry of this plate is shown in Fig.7 and its dimensions are: $b_1= b_2= b_4= b_5=L/6$, $b_3=L/3$ and $h=0.01L$. The stacking sequence is considered as $[+\langle 30/0\rangle,-\langle 30/0\rangle,+\langle 30/0\rangle]$ and the mechanical properties of this plate are the same as those of Plate 2 in Table 1. In this table, it could be seen how natural frequencies change by crank angles $\beta=150°$, $\beta=135°$ and $\beta=120°$, and boundary conditions SSSS, SFSF, SCSC and SCSF.

Table 10
The first four normalized frequencies of VSCL one-fold and two-fold folded plates.

stacking sequence	Mode	One-fold (NS=4, *n*=3)	Two-fold (NS=6, *n*=3)
$[\langle 30/0\rangle,\langle -30/0\rangle,\langle 30/0\rangle]$	1	0.13479	0.17279
	2	0.14776	0.18118
	3	0.36518	0.54373
	4	0.44550	0.57553
$[\langle 0/45\rangle,\langle 0/-45\rangle,\langle 0/45\rangle]$	1	0.18548	0.25667
	2	0.20340	0.26385
	3	0.48578	0.56857
	4	0.49640	0.60287
$[\langle 30/45\rangle,\langle -30/-45\rangle,\langle 30/45\rangle]$	1	0.17810	0.27893
	2	0.21035	0.29010
	3	0.44045	0.56825
	4	0.47976	0.60203

Table 11
The first four normalized frequencies of VSCL folded plates.

		Mode			
	Crank angle (β)	1	2	3	4
One-fold (NS=4, *n*=3)	90°	0.18473	0.20483	0.49371	0.49756
	120°	0.18475	0.20466	0.49368	0.49772
	150°	0.18476	0.20375	0.49347	0.49778
Two-fold (NS=6, *n*=3)	90°	0.25872	0.26771	0.56898	0.60275
	120°	0.25864	0.26676	0.56876	0.60246
	150°	0.25796	0.26169	0.56736	0.60066
Three-fold (NS=8, *n*=3)	90°	0.34081	0.34250	0.66351	0.69783
	120°	0.34397	0.34430	0.66464	0.69913
	150°	0.34332	0.34509	0.66495	0.69945
Four-fold (NS=12, *n*=3)	120°	0.43854	0.44205	0.64350	0.86956
	135°	0.48596	0.49377	0.63900	0.89256
	150°	0.50386	0.51281	0.61763	0.89997

Table 12
The first four normalized frequencies of VSCL four-fold folded plates (NS=12, *n*=3).

		Mode			
Crank angle(β)	Boundary condition	1	2	3	4
120°	SSSS	0.37939	0.60778	0.81083	0.84893
	SFSF	0.37612	0.38276	0.61250	0.81083
	SCSC	0.37941	0.60953	0.81083	0.84893
	SCSF	0.37941	0.60953	0.81083	0.84893
135°	SSSS	0.36520	0.59902	0.80682	0.84445
	SFSF	0.36224	0.36824	0.60371	0.80682
	SCSC	0.36523	0.60120	0.80682	0.84445
	SCSF	0.36523	0.60120	0.80682	0.84445
150°	SSSS	0.32965	0.56998	0.65866	0.77874
	SFSF	0.32749	0.33179	0.57866	0.65502
	SCSC	0.32968	0.57584	0.68413	0.79537
	SCSF	0.32968	0.57584	0.68413	0.79537

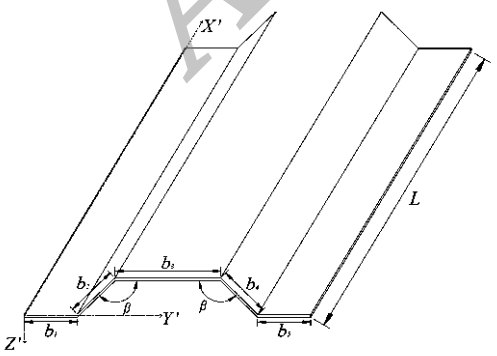

Fig.7
Geometrical properties of the four-fold folded plate.

In Fig.8, the effect of crank angle β on the fundamental frequency of VSCL four-fold folded plate for wide range of β from 0° to 180° is depicted. The geometry of this plate is shown in Fig.7 and its dimensions are: *L*=3m,

b_1= b_2= b_4= b_5=0.5m, b_3=1m and h=0.03m. The mechanical properties of this plate are the same as those of Plate 2 in Table 1. The stacking sequence is $[+\langle 0/T_1\rangle, -\langle 0/T_1\rangle, +\langle 0/T_1\rangle]$ and the boundary conditions are considered as SCSC.

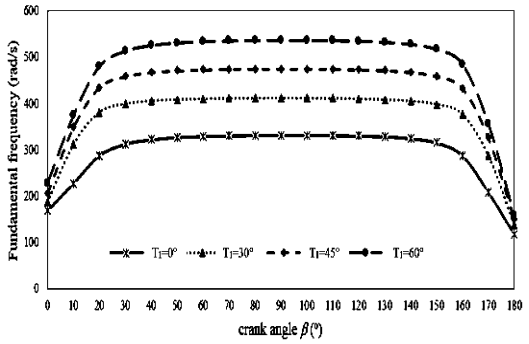

Fig.8
The effect of crank angle β on the fundamental frequency of a VSCL four-fold folded plate with stacking sequence $[+\langle 0/T_1\rangle, -\langle 0/T_1\rangle, +\langle 0/T_1\rangle]$.

The effect of length to thickness ratio (L/h) and the effect of E_1/E_2 ratio on the first frequency are depicted in Fig. 9 and Fig. 10, respectively. Here, one-fold (L=2m, b_1=b_2=L/2, β =120°), two-fold (L=2m, b_1=b_2=b_3=L/3, β =120°) and three-fold (L=2m, b_1=b_2=b_3=b_4=L/4, β =120°) folded plates are investigated. The geometry of the plates investigated corresponds to Fig. 5. The mechanical properties of these plates are: E_2=7.2Gpa, G_{12}=0.522E_2, ν_{12} =0.29 and ρ =1540kg/m^3. The results presented in Fig.9 and Fig.10 are calculated for E_1=24.08E_2 and h=0.01L, respectively. Moreover, the stacking sequence of these plates is considered as $[\langle 30/45\rangle, \langle -30/-45\rangle, \langle 30/45\rangle]$ and the boundary conditions are considered as SFSF. As seen in Fig. 9, as L/h ratio increases the fundamental frequency decreases, and, as the folding order increases the fundamental frequency increases. This is the reason why as L/h ratio increases the rigidity of the plate decreases, and as the folding order increases the rigidity of the plate increases.

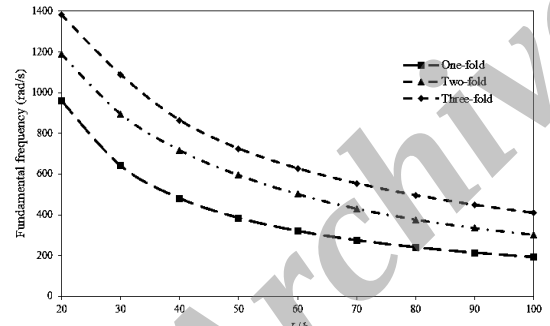

Fig.9
The effect of L/h ratio on the fundamental frequency for VSCL folded plates.

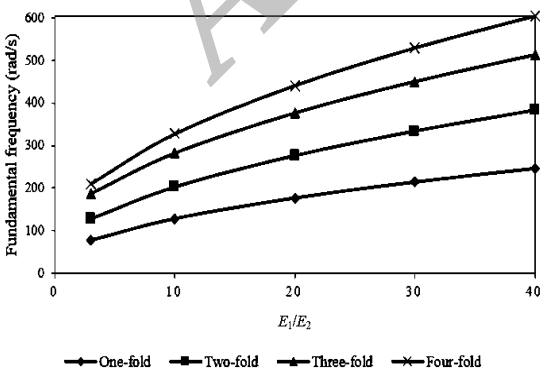

Fig.10
The effect of E_1/E_2 ratio on the fundamental frequency for VSCL folded plates.

4 CONCLUSIONS

In this study, natural frequencies of variable stiffness composite laminated (VSCL) flat and folded plates are presented. Most of the studies on VSCL flat plates are limited to their analysis with clamped boundary conditions or are based on the finite element method. In addition, there is no data in the field of VSCL folded plates analysis. In the present study, a semi-analytical finite strip method based on classical laminated plate theory is developed to study the free vibration of VSCL flat and folded plates. In this study, it was observed that in fully simply supported VSCL flat plate, by increasing the value of the angle of curvilinear fibers at the edges of plate T_1 and keeping constant the value of angle of curvilinear fibers at the center of plate T_0, the first natural frequencies increase. However, in fully clamped VSCL flat plate, by increasing T_1 and keeping T_0 constant, fundamental frequency decreases. Moreover, in VSCL folded plates, when the folding order increases, by changing the crank angle, more variation is created in the natural frequencies.

REFERENCES

[1] Akhavan H., Ribeiro P., 2011, Natural modes of vibration of variable stiffness composite laminates with curvilinear fibers, *Composite Structures* **93**(11): 3040-3047.

[2] Gürdal Z., Tatting B.F., Wu C.K., 2008, Variable stiffness composite panels: effects of stiffness variation on the in-plane and buckling response, *Composites: PartA* **39**: 911-922.

[3] Ribeiro P., Akhavan H., 2012, Non-linear vibrations of variable stiffness composite laminated plates, *Composite Structures* **94**: 2424-2432.

[4] Akhavan H., Ribeiro P., Moura M.F.S.F., 2013, Large deflection and stresses in variable stiffness composite laminates with curvilinear fibres, *International Journal of Mechanical Sciences* **73**: 14-26.

[5] Houmat A., 2013, Nonlinear free vibration of laminated composite rectangular plates with curvilinear fibers, *Composite Structures* **106**: 211-224.

[6] Yazdani S., Ribeiro P., Rodrigues J.D., 2014, A p-version layerwise model for large deflection of composite plates with curvilinear fibers, *Composite Structures* **108**: 181-190.

[7] Akbarzadeh A.H., Arian Nik M., Pasini D., 2014, The role of shear deformation in laminated plate with curvilinear fiber paths and embedded defects, *Composite Structures* **118**: 217-227.

[8] Yazdani S., Ribeiro P., 2015, A layerwise p-version finite element formulation for free vibration analysis of thick composite laminates with curvilinear fibres, *Composite Structures* **120**: 531-542.

[9] Reddy J.N., 2004, *Mechanics of Laminated Composite Plates and Shells: Theory and Analysis*, CRC Press, Boca Raton, FL, Second Edition.

[10] Hatami S., Azhari M., Saadatpour M.M., 2007, Free vibration of moving laminated composite plates, *Composite Structures* **80**: 609-620.

[11] Amoushahi H., Azhari M., 2013, Static analysis and buckling of viscoelastic plates by a fully discretized nonlinear finite strip method using bubble functions, *Composite Structures* **100**: 205-217.

[12] Cheung Y.K., 1976, *Finite Strip Method in Structural Analysis*, Pergamon Press, Oxford, Second Edition.

[13] Whitney J.M., 1987, *Structural Analysis of Laminated Anisotropic Plates*, Technomic Publishing Company Inc, Pennsylvania.

[14] Chow S.T., Liew K.M., Lam K.Y., 1992, Transverse vibration of symmetrically laminated rectangular composite plates, *Composite Structures* **20**(4): 213-226.

[15] Leissa A.W., Narita Y., 1989, Vibration studies for simply supported symmetrically laminated rectangular plates, *Composite Structures* **12**(2): 113-132.

[16] Dai K.Y., Liu G.R., Lim K.M., Chen X.L., 2004, A mesh-free method for static and free vibration analysis of shear deformable laminated composite plates, *Journal of Sound and Vibration* **269**: 633-652.

[17] Topal U., Uzman Ü., 2009, Frequency optimization of laminated folded composite plates, *Materials and Design* **30**(3): 494-501.

[18] Peng L.X., Kitipornchai S., Liew K.M., 2007, Free vibration analysis of folded plate structures by the FSDT mesh-free method, *Computational Mechanics* **39**(6): 799-814.

[19] Guha Niyogi A., Laha M.K., Sinha P.K., 1999, Finite element vibration analysis of laminated composite folded plate structures, *Shock and Vibration* **6**(5-6): 273-283.

[20] Le-Anh L., Nguyen-Thoi T., Ho-Huu V., Dang-Trung H., Bui-Xuan T., 2015, Static and frequency optimization of folded laminated composite plates using an adjusted Differential Evolution algorithm and a smoothed triangular plate element, *Composite Structures* **127**: 382-394.

[21] Lee S.Y., Wooh S.C., Yhim S.S., 2004, Dynamic behavior of folded composite plates analyzed by the third order plate theory, *International Journal of Solids and Structures* **41**(7): 1879-1892.

[22] Haldar S., Sheikh A.H., 2005, Free vibration analysis of isotropic and composite folded plates using a shear flexible element, *Finite Elements in Analysis and Design* **42**(3): 208-226.